

Supplemental Information

Tma64/eIF2D, Tma20/MCT-1, and Tma22/DENR

Recycle Post-termination 40S Subunits *In Vivo*

David J. Young, Desislava S. Makeeva, Fan Zhang, Aleksandra S. Anisimova, Elena A. Stolboushkina, Fardin Ghobakhloo, Ivan N. Shatsky, Sergey E. Dmitriev, Alan G. Hinnebusch, and Nicholas R. Guydosh

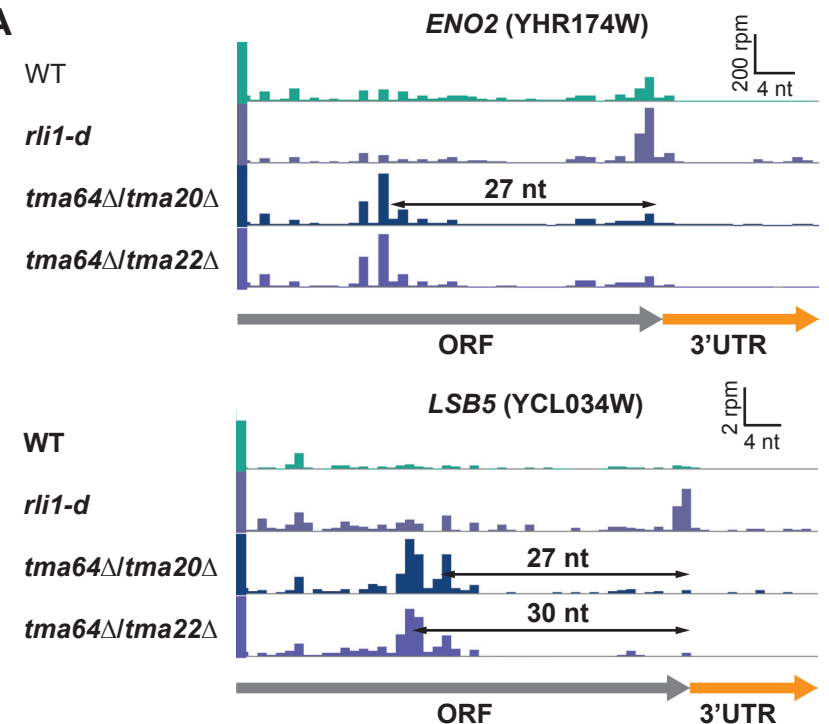
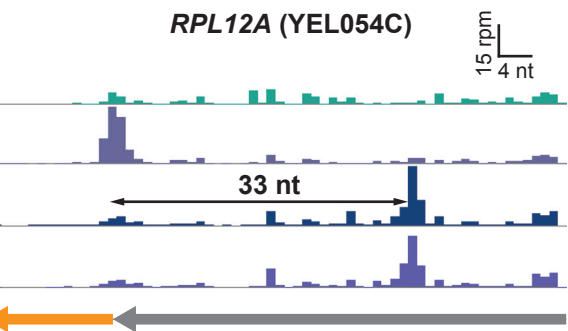
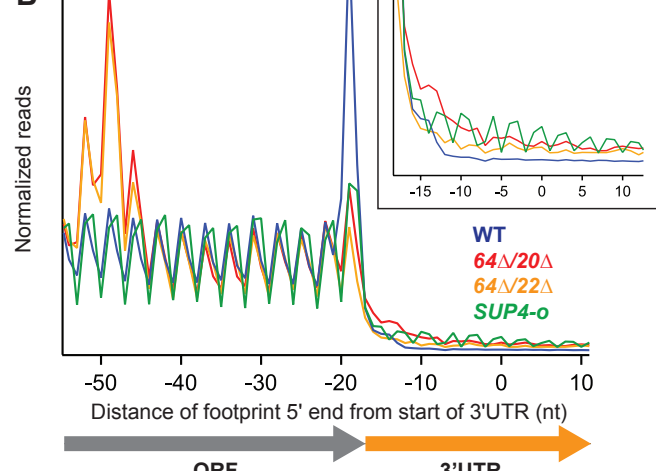
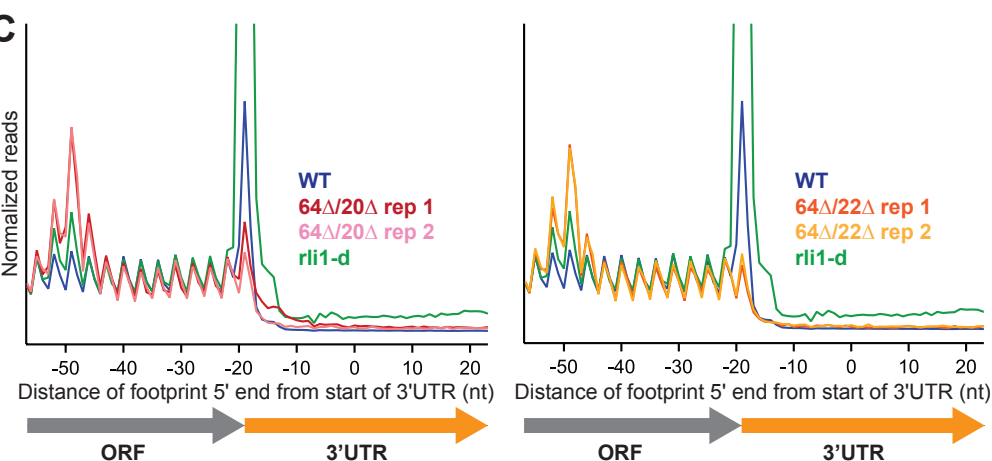
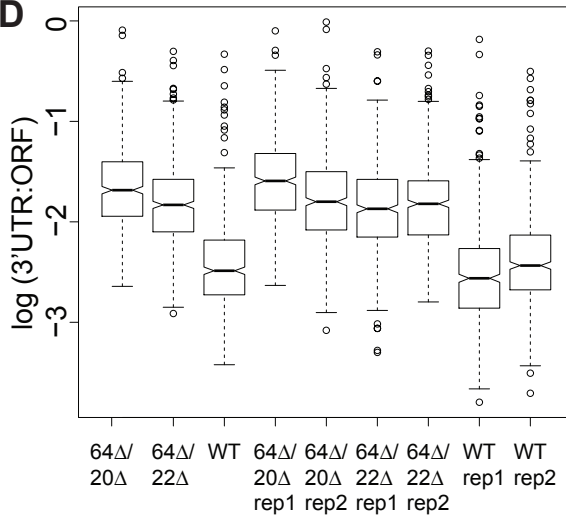
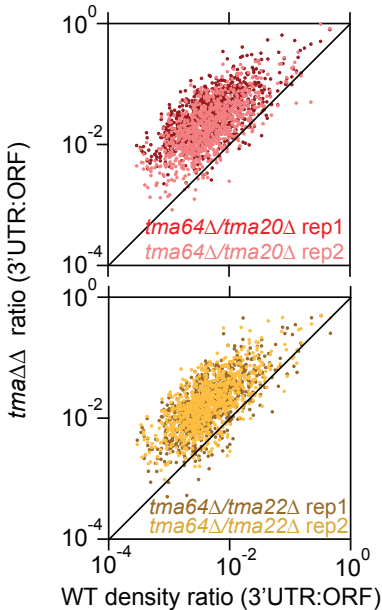
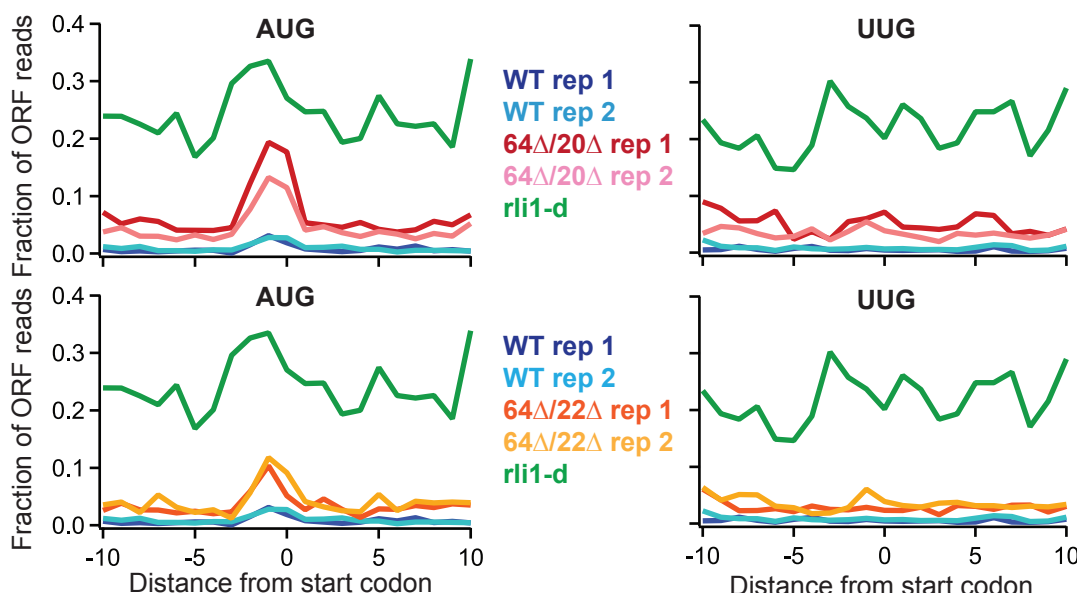
A**RPL12A (YEL054C)****B****C****D****E****F****Figure S1**

Figure S1. Analysis of queued ribosomes and 3'UTR reading frame in *tmaΔΔ* mutant strain ribosome profiling data. Related to Figures 1-2.

(A) Ribosome footprint profiles of genes *ENO2*, *RPL12A*, and *LSB5* showing ribosome occupancy peaks 27-33 nt upstream of the stop codon that represent stalled elongating 80S ribosomes. Reads are shifted so peaks approximately correspond to ribosome A sites.

(B) Normalized average ribosome footprint occupancy (each gene weighted equally) from all genes aligned at their stop codons for WT, *tma64Δ/tma20Δ*, *tma64Δ/tma22Δ*, and *SUP4-o* cells.

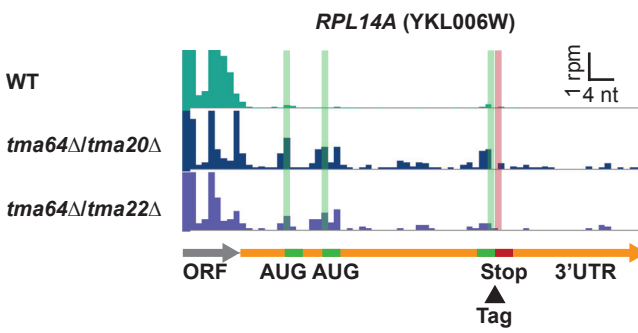
(Inset) Normalized average ribosome footprint occupancy for the first ~20 nt of the 3'UTRs of all genes for WT, *tma64Δ/tma20Δ*, *tma64Δ/tma22Δ*, and *SUP4-o* cells showing the absence of frame in the 3'UTR for *tma64Δ/tma20Δ*, *tma64Δ/tma22Δ*. This shows that these mutants do not generate a simple readthrough phenotype.

(C) Normalized average ribosome footprint occupancy (each gene weighted equally) from all genes aligned at their stop codons. Same as Fig. 1A but using data from two biological replicates for the *tma64Δ/tma20Δ* and *tma64Δ/tma22Δ* strains.

(D) Box plots of quantitated footprint data showing median log(10)-transformed 3'UTR:ORF ratios for datasets in Fig. 1D for individual replicates. All plots include data from the same set of genes ($N=543$) which were represented in all datasets. Boxes represent the interquartile range (IQR) and internal horizontal line represents the median. Whiskers represent $1.5 \times \text{IQR}$ and notches represent $1.58 \times \text{IQR} / \sqrt{N}$. For all comparisons, the median ratios are significantly higher in the mutant versus WT strains ($P < 2.2 \times 10^{-16}$, Mann-Whitney U test).

(E) Ratio of footprint densities in 3'UTRs to the respective ORFs. Same as for Fig. 1D but for replicate datasets from *tma64Δ/tma20Δ* and *tma64Δ/tma22Δ* strains.

(F) Average fraction of ribosome occupancy in a window surrounding 3'UTR AUG codons (left) and 3'UTR near-cognate UUG codons (right) normalized to ORF ribosome occupancy level (all frames included). Same as for Fig. 2B but for replicate datasets from WT, *tma64Δ/tma20Δ*, and *tma64Δ/tma22Δ* strains.

A***RPL14A* Stop**

```

[TAA] AAT [ATG] TAC [ATG] ATC TTT AAT TCT GAT
ATA TTT CGT [ATG] TAA TTT TAT CTT [TAA] CTG
GTG ATT CTT TTA ATA AAT AAA CTA CAA TAT

```

-AUG3

```

[TAA] AAT [ATG] TAC [ATG] ATC TTT AAT TCT GAT
ATA TTT CGT [AAA] TAA TTT TAT CTT [TAA] CTG
GTG ATT CTT TTA ATA AAT AAA CTA CAA TAT

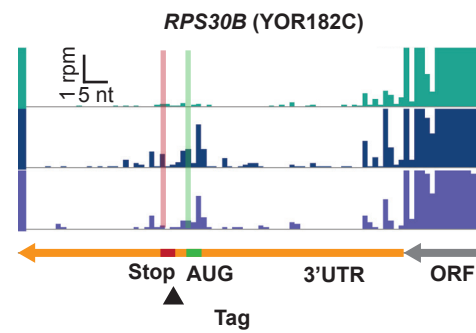
```

No AUG

```

[TAA] AAT [AAA] TAC [AAA] ATC TTT AAT TCT GAT
ATA TTT CGT [AAA] TAA TTT TAT CTT [TAA] CTG
GTG ATT CTT TTA ATA AAT AAA CTA CAA TAT

```

B***RPS30B* Stop**

```

[TAG] ATA CTA TCT [AAA] ATT CTA TAC TTT TAT
TGT TCT ACA [TGT] GTA ATT [AAA] CAA AAA TAT
TAT AAT [TAG] GAA ATA TTT ACC CTT TTT ACA

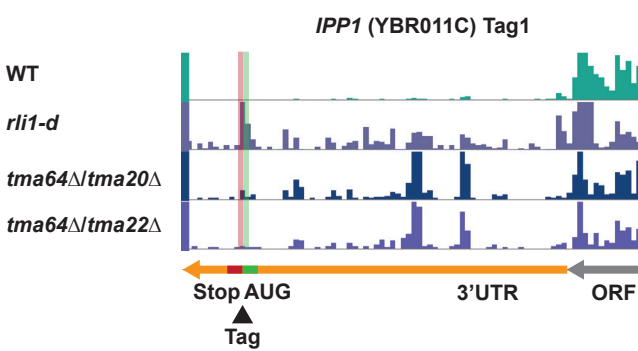
```

No AUG

```

[TAG] ATA CTA TCT [AAA] ATT CTA TAC TTT TAT
TGT TCT ACA [AAT] GTA ATT [AAA] CAA AAA TAT
TAT AAT [TAG] GAA ATA TTT ACC CTT TTT ACA

```

C***IPP1* Stop**

```

[TAA] AAT ATT TTG AAT [TGA] AAA [TGA] GAC ACC
TAC CAC GTA TGC GGC TTC AAG [TTG] TTT AAT
[ATG] [TAG] CTA TAT ATC GAT TAT ATA ACT GAC

```

No AUG

```

[TAA] AAT ATT TTG AAT [TGA] AAA [TGA] GAC ACC
TAC CAC GTA TGC GGC TTC AAG [AAA] TTT AAT
[AAA] [TAG] CTA TAT ATC GAT TAT ATA ACT GAC

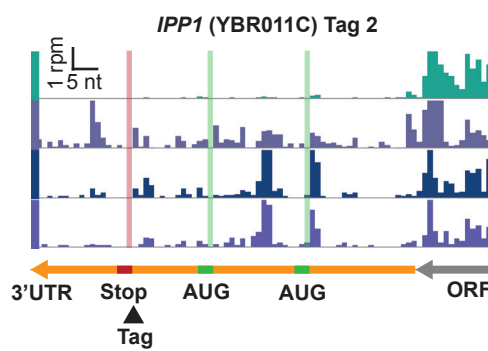
```

No NUG

```

[TAA] AAT ATT TTG AAT [TGA] AAA [TGA] GAC ACC
TAC CAC GTA TGC GGC TTC AAG [AAA] TTT AAT
[AAA] [TAG] CTA TAT ATC GAT TAT ATA ACT GAC

```

***IPP1* Stop**

```

[TAA] AAT ATT TTG AAT [TGA] AAA [TGA] GAC ACC
TAC CAC GTA TGC GGC TTC AAG TTG TTT AAT
[ATG] [TAG] CTA TAT ATC GAT TAT ATA ACT GAC

```

-AUG1

```

[TAA] AAT ATT TTG AAT [TGA] AAA [AAA] GAC ACC
TAC CAC GTA TGC GGC TTC AAG TTG TTT AAT
[ATG] [TAG] CTA TAT ATC GAT TAT ATA ACT GAC

```

-UUG -AUG1

```

[TAA] AAT ATT TTG AAA [AAA] AAA GAC ACC
TAC CAC GTA TGC GGC TTC AAG TTG TTT AAT
[ATG] [TAG] CTA TAT ATC GAT TAT ATA ACT GAC

```

-NUG

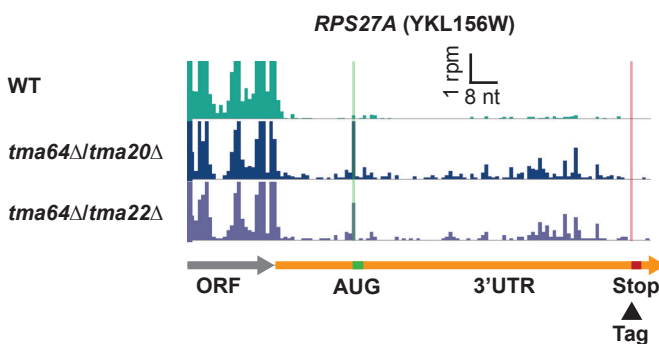
```

[TAA] AAT ATT TTG AAA [AAA] AAA GAC ACC
TAC CAC GTA AAC GGC TTC AAG TTG TTT AAT
[ATG] [TAG] CTA TAT ATC GAT TAT ATA ACT GAC

```

Figure S2

D

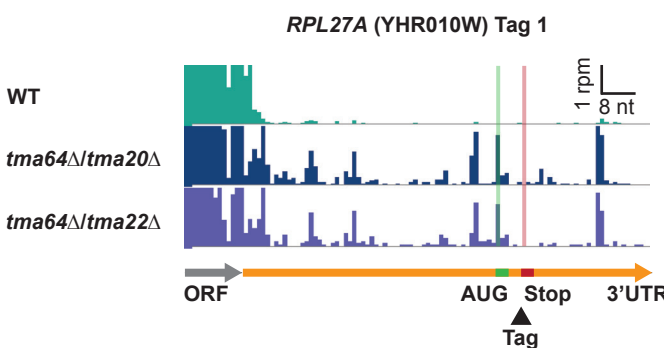
*RPS27A Stop*

TAA TTT CAT TAC TAG ACA GAT GAA ACG AAA
TTT ACT TCA AAA GAA GAG CAT TAA TAA AGT
GAT TCA ATT ATG GAA CCA GCA GGG TAG GTT
TTA TCA TAT ATA TAC ACT

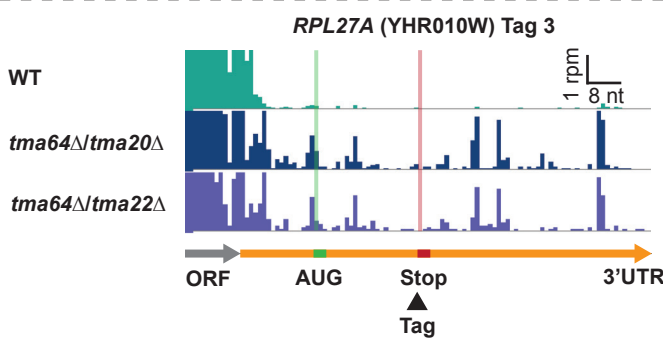
No AUG

TAA TTT CAT TAC TAG ACA GAA AAA ACG AAA
TTT ACT TCA AAA GAA GAG CAT TAA TAA AGT
GAT TCA ATT ATG GAA CCA GCA GGG TAG GTT
TTA TCA TAT ATA TAC ACT

F

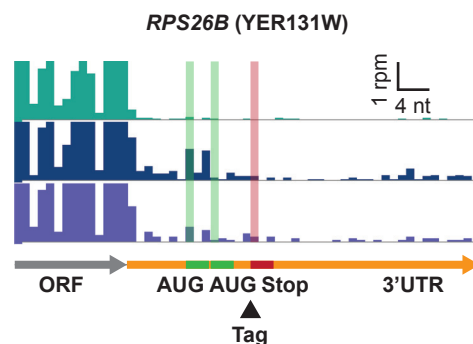
*RPL27A Stop*

TAA GAG AAT TGC ATT ATG GTC AAC CAA AAA
TCA AAA AAT TAT TAG TAA TAT CAA CAT ATG
TAT ATT TAA TGT ATG TAA ACA ATG ATT AAA
TAT TAA TAA AAT ATA

*RPL27A Stop*

TAA GAG AAT TGC ATT ATG GTC AAC CAA AAA
TCA AAA AAT TAT TAG TAA TAT CAA CAT ATG
TAT ATT TAA TGT ATG TAA ACA ATG ATT AAA
TAT TAA TAA AAT ATA

E

*RPS26B Stop*

TAA ATA TGA TGA GAG AAT AAT ATA AAT CAA
ACG CTC GCT GAT TAA GGT GTC ATT TAT TTT
TTT TAA TAG AGG CTT TGT CTT TTA TAA TTG

-AUG1

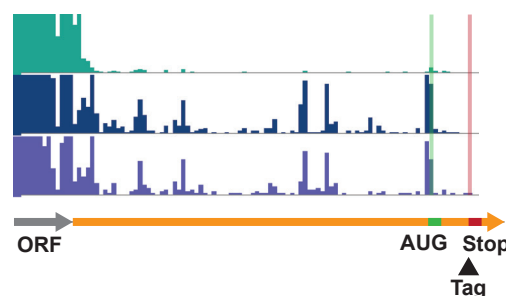
TAA ATA AAA TGA GAG AAT AAT ATA AAT CAA
ACG CTC GCT GAT TAA GGT GTC ATT TAT TTT
TTT TAA TAG AGG CTT TGT CTT TTA TAA TTG

-AUG2

TAA ATA TGA AAA GAG AAT AAT ATA AAT CAA
ACG CTC GCT GAT TAA GGT GTC ATT TAT TTT
TTT TAA TAG AGG CTT TGT CTT TTA TAA TTG

No AUG

TAA ATA AAA AAA GAG AAT AAT ATA AAT CAA
ACG CTC GCT GAT TAA GGT GTC ATT TAT TTT
TTT TAA TAG AGG CTT TGT CTT TTA TAA TTG

RPL27A (YHR010W) Tag 2*RPL27A Stop*

TAA GAG AAT TGC ATT ATG GTC AAC CAA AAA
TCA AAA AAT TAT TAG TAA TAT CAA CAT ATG
TAT ATT TAA TGT ATG TAA ACA ATG ATT AAA
TAT TAA TAA AAT ATA

No AUG

TAA GAG AAT TGC ATT AAA GTC AAC CAA AAA
TCA AAA AAT TAT TAG TAA TAT CAA CAT ATG
TAT ATT TAA TGT ATG TAA ACA ATG ATT AAA
TAT TAA TAA AAT ATA

Figure S2

Figure S2. Candidate genes and epitope-tagged reporter constructs used to investigate 3'UTR reinitiation in the *tmaΔΔ* strains, related to Figure 3.

Ribosome footprint profiles of the 3'UTRs of genes *RPL14A* (A), *RPS30B* (B), *IPPI* tag 1 and 2 (C), *RPS27A* (D), *RPS26B* (E), and *RPL27A* tag 1, 2, and 3 (F) showing ribosome occupancy peaks at 3'UTR AUG codons. Green line and bars represent AUG start codon(s) and red lines and bars represent stop codons in the same frame. Gene annotations are drawn to correspond to data for ribosome P sites (AUG codons) or A sites (stop codons). Note that the 3rd AUG and stop codon for *RPL14A* are slightly offset for visibility. The sites of insertion of the MYC13 epitope tags just upstream of the 3'UTR stop codons is highlighted by black triangles. A portion of the 3'UTR sequences are shown, highlighting the main ORF stop codon (filled grey boxes), 3'UTR AUG start codons (green boxes), in-frame 3'UTR stop codons (relative to the AUGs; pink boxes), and out-of frame 3'UTR start and stop codons (dotted boxes). The tagged candidate genes were cloned onto high copy plasmids. Reporter constructs were subjected to site-directed mutagenesis to change in-frame AUG and UUG codons to AAA codons to test if the observed reinitiation products arose from 40S initiation. Nucleotides mutated to remove AUG and near-cognate start codons are highlighted in red for each reporter construct.

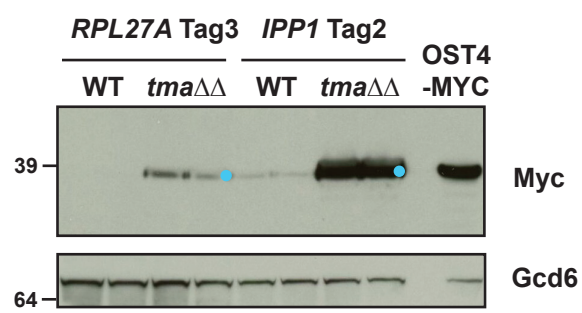
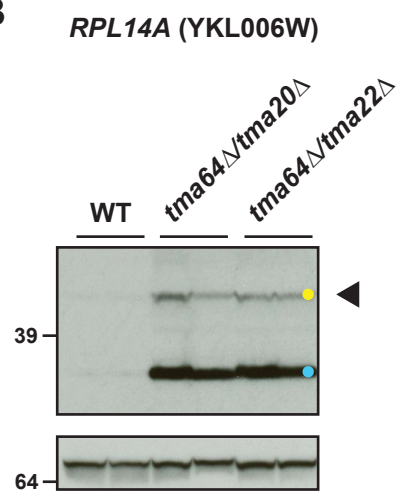
A**B**

Figure S3

Figure S3. Detection of epitope-tagged 3'UTR translation products in the *tma* deletion strains, related to Figure 3.

- (A)** Western analysis was carried out as in Figure 3A. 3'UTR reinitiation products are marked with cyan dots.
- (B)** The putative read-through product expressed from the *RPL14A* reporter is expressed at comparable levels in both *tmaΔΔ* strains (arrowhead). The 3'UTR reinitiation product is marked with a cyan dot and the readthrough/frameshift product is marked with a yellow dot. In all panels, if not stated otherwise, at least 2 biological replicates were used to ensure effects were reproducible.

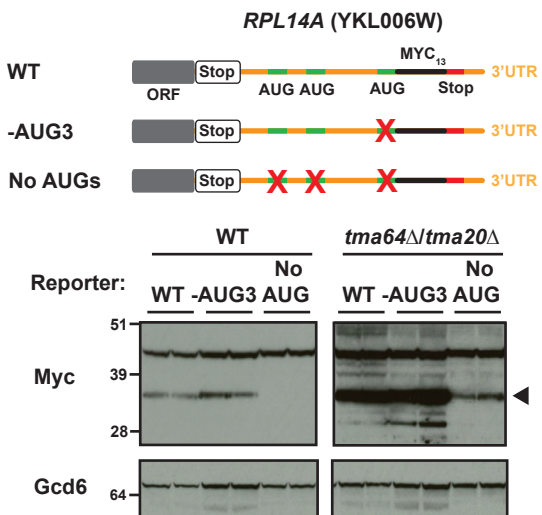
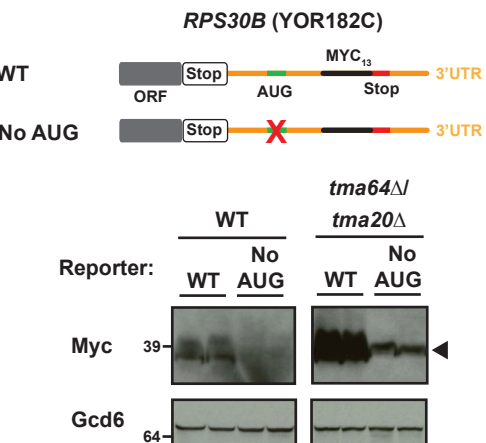
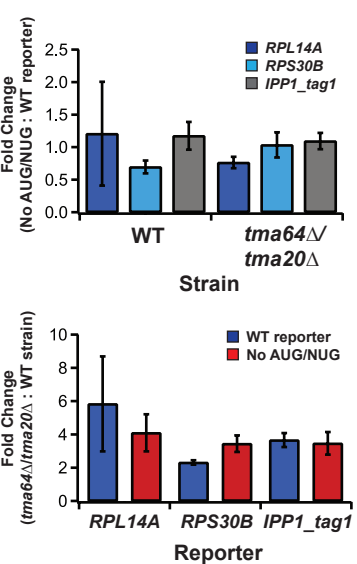
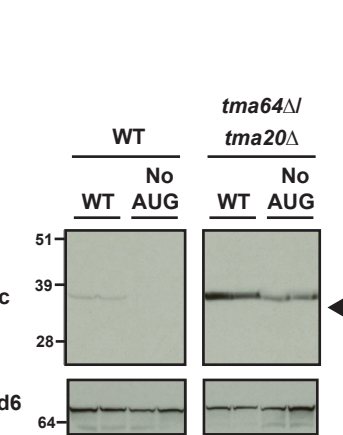
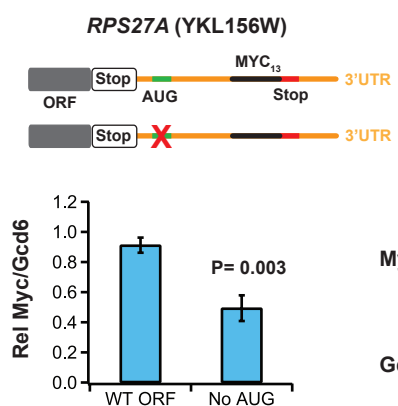
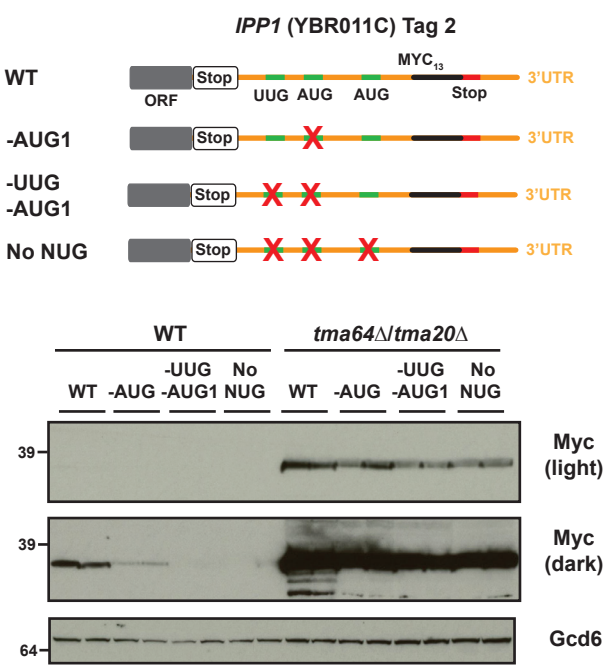
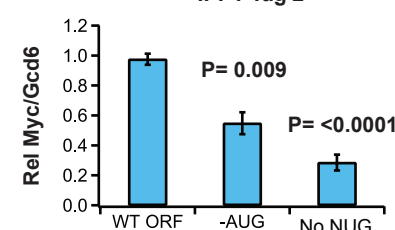
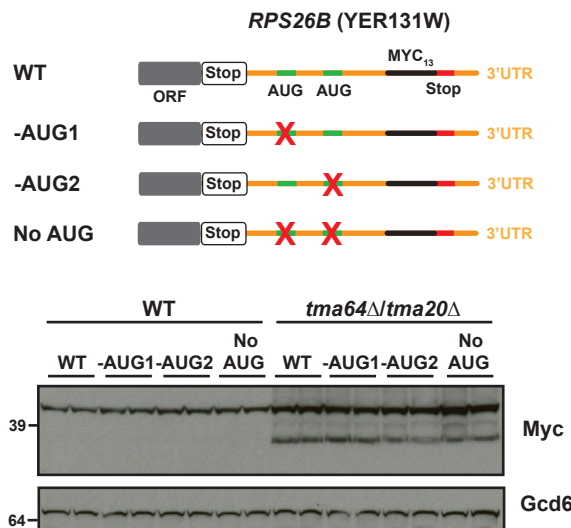
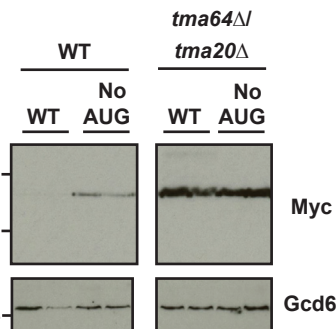
A**B****C****D****E****F****G****Figure S4**

Figure S4. Further examples of 3'UTR translation products resulting from 40S and 80S reinitiation in the *tma* deletion strains, related to Figure 3.

Western analysis was carried out as in Figure 3B-E.

(A and B) Darker exposures of the western blots for *RPL14A* (A) and *RPS30B* (B) shown in Figure 3A and B showing that in WT cells AUG mutations in these two reporters eliminate or reduce expression of the reinitiation products similar to what is observed in *tmaΔΔ* cells.

(C) BY4741(WT) and *tma64Δ/tma20Δ* strains carrying WT reporter plasmids for *RPL14A* (pLfz609-1), *RPS30B* (pLfz606-1), and *IPPI_tag1* (pLfz610-1), or a matching set (defined as “No AUG/NUG”) of mutant reporters lacking all AUG codons that could potentially be used for reinitiation in *RPL14A* (pLfz609-NoAUG) and *RPS30B* (pLfz606-NoAUG) or both AUG and UUG codons that could potentially be used for reinitiation in *IPPI_tag1* (pLfz610-NoNUG), were grown in SC-U to an OD₆₀₀ of 0.8-1.0.

Total RNA was purified from three cultures for each strain/reporter combination and reporter mRNA levels were quantified in triplicate by qRT-PCR and normalized to the level of *ACT1* mRNA. Data from the three biological replicates are reported as mean ± standard deviation. **(Left)** Fold-change of the “No AUG/NUG” reporter to the WT reporter in WT and *tma64Δ/tma20Δ* strains. There is no increase in mRNA abundance for the “No AUG/NUG” variants compared to the corresponding WT reporters in either strain. **(Right)** Fold-change of each reporter between the *tma64Δ/tma20Δ* strain and the BY4741(WT) strain. The mRNA level of each reporter was increased by 2-4-fold in the *tma64Δ/tma20Δ* strain relative to the WT strain (far less than the observed differences in protein levels), which might result from their increased translation in the mutant cells as

translation efficiency is an important determinant of mRNA stability in yeast (Schwartz and Parker 1999; LaGrandeur and Parker 1999).

(D) Mutation of the AUG codon predicted to serve as a reinitiation start codon in the 3'UTR of *RPS27A* conferred a significant, albeit partial reduction in expression of the putative reinitiation product by ~50%. The graph contains averaged data for ten independent cultures (both stationary and exponential cultures) for each reporter construct in the *tmaΔΔ* strain obtained from four separate Western blots, including that shown on the left. Error bars are +/- S.E.M. The amount of reinitiation product was significantly lower in the No AUG *RPS27A* construct relative to the WT *RPS27A* construct ($P = 0.003$, 2-tailed students T-test).

(E) Mutation of the AUG codon predicted to serve as a reinitiation start codon in the 3'UTR of the *IPPI_tag2* reporter reduced expression of the putative reinitiation product by only ~50% A greater reduction occurred when an upstream in-frame UUG and downstream in-frame AUG were also mutated indicating that reinitiation can occur at more than one AUG or near-cognate start codon in the 3'UTR of this gene. The graph contains averaged data for four independent cultures for each construct in the *tmaΔΔ* strain obtained from two separate Western blots. Error bars are +/- S.E.M. The reinitiation product abundance was significantly lower in the -AUG *IPPI_tag2* construct relative to the WT *IPPI_tag2* construct ($P = 0.009$, 2-tailed students T-test), and even further reduced in the No NUG construct ($P=<0.0001$, 2-tailed students T-test).

(F and G) Mutation of the 3'UTR AUGs in the *RPS26B* (F) and *RPL27A_tag 3* (G) reporters did not result in loss of the 3'UTR reinitiation product suggesting that it is the

result of 80S reinitiation. In all panels, if not stated otherwise, at least 2 biological replicates were used to ensure effects were reproducible.

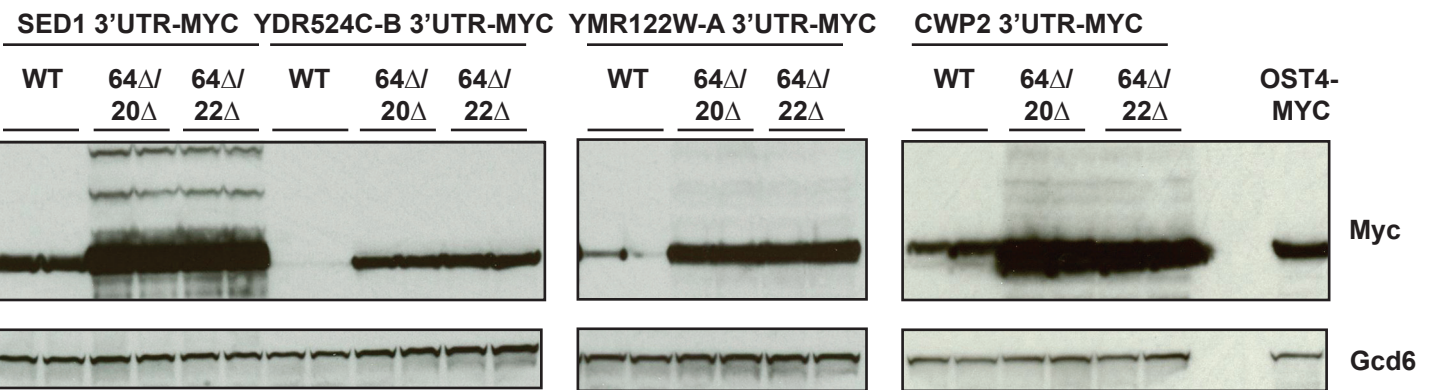


Figure S5

Figure S5. Detection of 80S reinitiation in the 3'UTRs of the *tma* deletion strains.

Related to Figure 3.

MYC₁₃-tagged reporters that had previously been used to detect 80S reinitiation in the 3'UTR of Rli1-depleted cells (Young et al., 2015) were cloned onto high copy plasmids and used to detect 80S reinitiation in the *tmaΔΔ* strains. Western analysis was carried out as in Figure 3A. In all panels, if not stated otherwise, at least 2 biological replicates were used to ensure effects were reproducible.

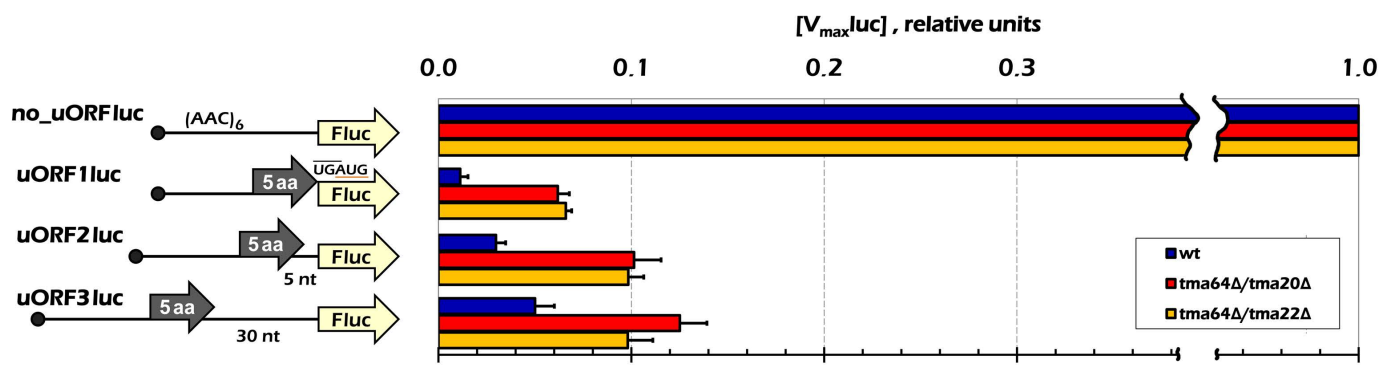
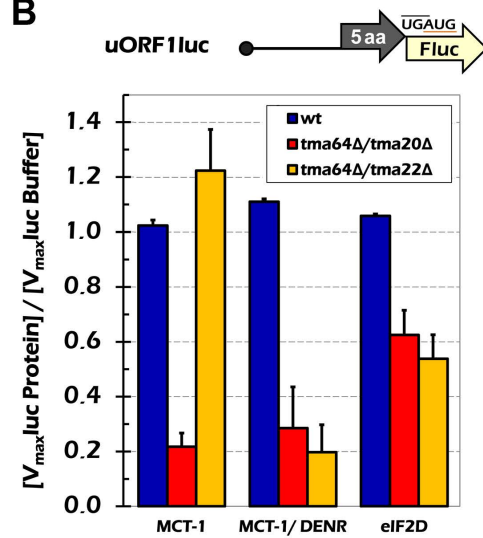
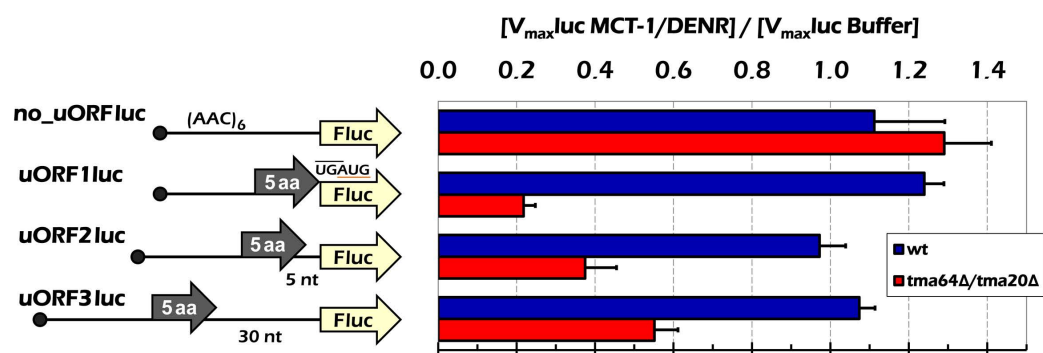
A**B****C****Figure S6**

Figure S6. Analysis of *in vitro* reinitiation data prior to complete normalization and effects of human MCT-1, MCT-1/DENR and eIF2D in complementing defects of missing yeast factors. Related to Figure 4.

(A) Levels of luciferase activity, normalized to the no_uORFluc construct (but without the ratio to WT lysate calculated) are shown for double mutant and WT lysates for the constructs analyzed in Fig. 4A. All of the uORFs present reduced Fluc expression by an order of magnitude or more compared to expression from the uORF-less construct (no_uORFluc) in WT lysate (note the break in the axis). Increasing the intercistronic distance from 0 to either 5 nt or 30 nt progressively diminishes the inhibitory effect of the uORF on Fluc expression in WT lysate (blue bars for uORF1luc vs. uORF2luc & uORF3luc), in accordance with a canonical 40S reinitiation mechanism. In the lysates missing the Tma proteins (red, orange bars), the relative changes in this trend are much weaker. (B) Effects of addition of purified recombinant MCT-1 or MCT-1/DENR dimer, or native eIF2D from HeLa cells, on uORF1luc mRNA translation in cell-free systems prepared from WT and double mutant knockout yeast strains. Maximal rates of luciferase accumulation were calculated, as described in Fig. 4A, right panel. These data show that the human homologs of yeast Tma20, Tma22, and Tma64 can serve as functional substitutes in yeast extract. (C) A broader set of uORF-containing mRNAs were translated in WT and *tma64Δtma20Δ* yeast lysates with and without the recombinant MCT-1/DENR dimer added. Maximal rates of luciferase accumulation were calculated, as described in Fig. 4A, right panel, demonstrating further that, like recombinant yeast protein, human protein can complement the apparent 40S recycling defect. For all panels,

3 replicates each containing 2 or more mRNA preparations were used for each experiment and error bars, mean \pm SD.

Table S1: Yeast Strains used in this study, related to STAR Methods.

Yeast Name	Genotype	3'UTR Tag Name	Myc Tag Position*	Source
BY4741	<i>MATA his3Δ1 leu2Δ0 met15Δ0 ura3Δ0</i>			Dharmacon
4051	<i>MATA his3Δ1 leu2Δ0 met15Δ0 ura3Δ0 tma64Δ::KanMX4</i>			Dharmacon
328	<i>MATA his3Δ1 leu2Δ0 met15Δ0 ura3Δ0 tma20Δ::KanMX4</i>			Dharmacon
6812	<i>MATA his3Δ1 leu2Δ0 met15Δ0 ura3Δ0 tma22Δ::KanMX4</i>			Dharmacon
FZY793	<i>MATA his3Δ1 leu2Δ0 met15Δ0 ura3Δ0 tma64Δ::HygMX4</i>			This study
YDY10	<i>MATA his3Δ1 leu2Δ0 met15Δ0 ura3Δ0 tma64Δ::HygMX4 tma20Δ::KanMX4</i>			This study
YDY12	<i>MATA his3Δ1 leu2Δ0 met15Δ0 ura3Δ0 tma64Δ::HygMX4 tma22Δ::KanMX4</i>			This study
YDY14	<i>MATA his3Δ1 leu2Δ0 met15Δ0 ura3Δ0 HIS3MX6::P_{GAL1}-SUI1</i>			This study
YDY26	<i>MATA his3Δ1 leu2Δ0 met15Δ0 ura3Δ0 tma64Δ::HygMX4 tma20Δ::KanMX4 HIS3MX6::P_{GAL1}-SUI1</i>			This study
YDY231	<i>MATA his3Δ1 leu2Δ0 met15Δ0 ura3Δ0 OST4-MYC13::HIS3MX6</i>			(Young et al. 2015)
FGY13	<i>MATA his3Δ1 leu2Δ0 met15Δ0 ura3Δ0 RPL27A-3'UTR-Tag1-MYC13::HIS3MX6</i>	RPL27A-Tag1	+64	This study
FGY25	<i>MATA his3Δ1 leu2Δ0 met15Δ0 ura3Δ0 tma64Δ::HygMX4 tma20Δ::KanMX4 RPL27A-3'UTR-Tag2-MYC13::HIS3MX6</i>	RPL27A-Tag2	+91	This study
FZY849	<i>MATA his3Δ1 leu2Δ0 met15Δ0 ura3Δ0 RPL27A-3'UTR-Tag3-MYC13::HIS3MX6</i>	RPL27A-Tag3	+40	This study
FGY39	<i>MATA his3Δ1 leu2Δ0 met15Δ0 ura3Δ0 RPS30B-3'UTR-Tag1-MYC13::HIS3MX6</i>	RPS30B-Tag1	+45	This study
FGY42	<i>MATA his3Δ1 leu2Δ0 met15Δ0 ura3Δ0 RPL14A-3'UTR-Tag1-MYC13::HIS3MX6</i>	RPL14A-Tag1	+40	This study
FGY31	<i>MATA his3Δ1 leu2Δ0 met15Δ0 ura3Δ0 RPS27A-3'UTR-Tag1-MYC13::HIS3MX6</i>	RPS27A-Tag1	+98	This study
FGY47	<i>MATA his3Δ1 leu2Δ0 met15Δ0 ura3Δ0 tma64Δ::HygMX4 tma20Δ::KanMX4 RPS26B-3'UTR-Tag1-MYC13::HIS3MX6</i>	RPS26B-Tag1	+15	This study
FGY57	<i>MATA his3Δ1 leu2Δ0 met15Δ0 ura3Δ0 IPP1-3'UTR-Tag1-MYC13::HIS3MX6</i>	IPP1-Tag1	+61	This study
FZY850	<i>MATA his3Δ1 leu2Δ0 met15Δ0 ura3Δ0 IPP1-3'UTR-Tag2-MYC13::HIS3MX6</i>	IPP1-Tag2	+54	This study
YDY104	<i>MATA his3Δ1 leu2Δ0 met15Δ0 ura3Δ0 SED1-3'UTR-MYC13::HIS3MX6</i>			(Young et al. 2015)
YDY106	<i>MATA his3Δ1 leu2Δ0 met15Δ0 ura3Δ0 YDR524C-B-3'UTR-MYC13::HIS3MX6</i>			(Young et al. 2015)
YDY108	<i>MATA his3Δ1 leu2Δ0 met15Δ0 ura3Δ0 CWP2-3'UTR-MYC13::HIS3MX6</i>			(Young et al. 2015)

Yeast Name	Genotype	3'UTR	Tag Name	Myc Tag Position*	Source
YDY132	<i>MATa his3Δ1 leu2Δ0 met15Δ0 ura3Δ0</i> <i>YMR122W-A-3'UTR-MYC13::HIS3MX6</i>				(Young et al. 2015)

* The positions of the MYC13 tags are relative to stop codon, with the first nucleotide after the stop codon numbered +1.

Table S3: Plasmids used in this study, related to STAR Methods.

Plasmid	Description	Source
pAG32	pFA6-hphMX4; HPH tagging cassette	(Goldstein and McCusker 1999)
pFA6a-His3MX6-PGAL1	P_{GAL1} promoter tagging cassette	(Longtine et al. 1998)
pJCB101	sc ¹ <i>LEU2 SUI1</i> in YCplac111	(Martin-Marcos, Cheung, and Hinnebusch 2011)
pPMB03	sc <i>LEU2 sui1-L96P</i> in YCplac111	(Martin-Marcos, Cheung, and Hinnebusch 2011)
pFA6a-13Myc-His3MX6	<i>MYC₁₃</i> tagging cassette	(Longtine et al. 1998)
YEplac195	hc ¹ <i>URA3</i>	(Gietz and Sugino 1988)
pET33b-MCTS1	Human MCT-1 untagged	(Lomakin et al. 2017)
pET33b-DENR	Human DENR untagged	(Lomakin et al. 2017)
pSV40-Fluc	pGL3-based luciferase plasmid	(Dmitriev et al. 2007)
pRFluc1fus	pYDL-based luciferase plasmid	a gift from Dr. I.Osterman (MSU)
pRFluc2	pYDL-based luciferase plasmid	a gift from Dr. I.Osterman (MSU)
pRFluc3	pGL3-based dual luciferase plasmid	pRF from (Dmitriev et al. 2007)
pET11c-TMA20	Yeast TMA20 untagged	This study
pET11c-TMA22	Yeast TMA22 untagged	This study

¹sc, single-copy; hc, high-copy

Table S4: High copy reporter plasmids used in this study, related to STAR Methods.

Plasmid Name	3'UTR Name / Myc Tag Position*	Reporter Mutations**
pLfz600	RPL27A-Tag1 / +64	Wild type
pLfz601	RPL27A-Tag2 / +91	Wild type
pLfz607	RPL27A-Tag2 / +91	Wild type
pLfz612-3	RPL27A-Tag3 / +40	Wild type
pLfz612-NoAUG	RPL27A-Tag3 / +40	UG+14, +15AA
pLfz605-3	RPS30B-Tag1 / +45	Wild type
pLfz605-NoAUG	RPS30B-Tag1 / +45	UG+37, +38AA
pLfz609-1	RPL14A-Tag1 / +40	Wild type
pLfz609-minusAUG3	RPL14A-Tag1 / +40	UG+38, +39AA
pLfz609-NoAUG	RPL14A-Tag1 / +40	UG+6, +7AA, UG+11, +12AA, UG+38, +39AA
pLfz602-1	RPS27A-Tag1 / +98	Wild type
pLfz602-NoAUG	RPS27A-Tag1 / +98	UG+18, +19AA
pLfz606-1	RPS26B-Tag1 / +15	Wild type
pLfz606-minusAUG1	RPS26B-Tag1 / +15	UG+4, +5AA
pLfz606-minusAUG2	RPS26B-Tag1 / +15	UG+7, +8AA
pLfz606-NoAUG	RPS26B-Tag1 / +15	UG+4, +5AA, UG+7, +8AA
pLfz610-1	IPP1-Tag1 / +61	Wild type
pLfz610-NoAUG	IPP1-Tag1 / +61	UG+59, +60AA
pLfz610-NoNUG	IPP1-Tag1 / +61	UUG+49 to +51AAA, UG+59, +60AA
pLfz611-3	IPP1-Tag2 / +54	Wild type
pLfz611-minusAUG1	IPP1-Tag2 / +54	UG+19, +20AA
pLfz611-minusUUG minusAUG1	IPP1-Tag2 / +54	UUG+12 to +14AAA, UG+19, +20AA
pLfz611-NoNUG	IPP1-Tag2 / +54	UUG+12 to +14AAA, UG+19, +20AA, UG+37, +38AA
pDY98	SED1 / +146	Wild type
pDY100	YDR524C-B / +138	Wild type
pDY101	CWP2 / +62	Wild type
pDY105	YMR122W-A / +59	Wild type

* The positions of the MYC13 tags are relative to stop codon, with the first nucleotide after the stop codon numbered +1.

** The position of substituted 3'UTR nucleotides are relative to the stop codon, with first nucleotide after the stop codon as +1.

Table S5: Read preparation and alignment statistics, related to STAR Methods.

Sample name	Description	Reads with linker	Not aligned to ncRNA	Aligned to genome or splice jcn
68F	tma20Δ_rep1	28,789,705	13,644,151	11,042,568
69F	tma20Δ_rep2	26,893,265	13,580,936	11,207,667
70F	tma22Δ_rep1	20,752,938	9,461,945	7,737,000
71F	tma22Δ_rep2	27,258,149	12,783,074	10,272,671
DJY07_1	SUI1_rep1	38,741,005	17,448,380	14,303,682
DJY08_1	SUI1_rep2	45,628,449	22,326,606	18,335,023
DJY07_2	sui1-l96p_rep1	37,776,774	17,281,419	13,977,463
DJY08_2	sui1-l96p_rep2	33,516,356	13,034,607	10,466,269
DJY07_3	tma22Δ/SUI1_rep1	38,751,952	18,148,550	14,987,877
DJY08_3	tma22Δ/SUI1_rep2	33,009,022	17,147,009	14,126,699
DJY07_4	tma22Δ/sui1-l96p_rep1	39,924,020	20,158,823	16,497,484
DJY08_4	tma22Δ/sui1-l96p_rep2	39,889,630	22,293,501	16,901,656
DJY09_1	wt_rep1	57,878,331	25,688,334	20,602,342
DJY10_1	wt_rep2	51,463,564	30,419,785	24,380,849